Electronic Supplementary Material (ESI) for Journal of Materials Chemistry A.

Mass Production of Dealloyed Pt_3Co/C Catalyst for Oxygen Reduction Catalysis in PEMFC

Yanhui Liu[a], Changhong Zhan[a], Juntao Zhang[a], Xiaoqing Huang[a,*] and Lingzheng Bu[b,*]

a. State Key Laboratory of Physical Chemistry of Solid Surfaces, College of Chemistry and Chemical Engineering, Xiamen University, Xiamen, 361005, China.

b. College of Energy, Xiamen University, Xiamen, 361102, China.

Experimental Procedures

1.1 Chemicals.

Platinum (II) acetylacetonate ($Pt(acac)_2$) was purchased from Sino-Precious Metals Holding Co., Ltd. Basic cobalt (II) carbonate hydrate ($2CoCO_3 \cdot 3Co(OH)_2$), zincnitrate hexahydrate ($Zn(NO_3)_2 \cdot 6H_2O$), formaldehyde aqueous solution, ethylene glycol and acetic acid were purchased from Sinopharm Chemical Reagent Co., Ltd. Cobalt (II) acetylacetonate ($Co(acac)_2$), cobalt (III) acetylacetonate ($Co(acac)_3$), cobalt acetate ($Co(Ac)_2$), nickel (II) acetylacetonate ($Ni(acac)_2$) and copper acetylacetonate ($Cu(acac)_2$) were purchase from Sigma-Aldrich. Commercial Pt/C (40 wt.% Pt) was purchased from Johnson Matthey. Amorphous carbon (C, Vulcan XC-72R) was purchased from Cabot.

1.2 Characterization.

The transmission electron microscopy (TEM) samples were prepared by dropping ethanol dispersion of samples on carbon-coated copper grids and dried under ambient condition. Low-magnification TEM was operated on JEM-1400 with an accelerating voltage of 100 kV. The high-resolution TEM (HRTEM) and scanning transmission electron microscopy energy dispersive spectroscopy (HAADF-STEM-EDS) was conducted on a FEI Tecnai F30 TEM at an accelerating voltage of 300 kV. X-ray diffraction (XRD) patterns were collected on a Smart Lab-SE powder diffractometer equipped with a Cu radiation source (λ = 0.15406 nm). Scanning electron microscopy EDS (SEM-EDS) was taken by ZEISS Sigma 300 field emission scanning electron microscope. The X-ray photoelectron spectroscopy spectra (XPS) were collected by XPS (Thermo Scientific, ESCALAB 250 XI). The carbon peak at 284.8 eV was used as the reference to correct for charging effects. The yield of Pt was determined by the ICP-OES (ICAP 7000, Thermo Fisher Scientific, Waltham, MA USA).

1.3 Synthesis of Pt_3Co-based nanoparticles on carbon support.

Different Pt_3Co/C catalysts are directly synthesized by one-pot method with the help of carbon support. The concentration of synthetic solution is adjustable, and we can synthesize 40 mg catalyst per milliliter of solvent. The synthesis process of Pt_3Co/C is as follows. $Pt(acac)_2$ (50 mg), $2CoCO_3 \cdot 3Co(OH)_2$ (13 mg), and Vulcan XC-72R C (50 mg) were added to 5 mL ethylene glycol. Then, 100 μL formaldehyde solution was added after ultrasonication. The resulting mixture was stirred and heated at 200°C for 10 h. After the solvent was cooled, the products were collected by centrifugation for twice and washed with 1 mol/L acetic acid solution. Then the pure acetic acid was added to the products, and the solution was heated at 80 °C for 24 h. The catalyst was collected by centrifugation and washed with 1 mol/L acetic

acid solution again. The catalyst was then dried at 90°C, grounded to powder, and annealed at 250°C for 2 h. The resulting D-Pt_3Co/C was collected for testing. The synthetic conditions of PtCo-3:1/C and PtCo-1:2/C are similar to those of PtCo-1:1/C except for using different amounts of $2CoCO_3{\cdot}3Co(OH)_2$ (4.5 mg and 26 mg). The PtCo/C-H_2PtCl_6 catalyst was synthesized by same method except for using the same molar weight of H_2PtCl_6 to replace $Pt(acac)_2$. The PtCo-$Co(Ac)_2$/C, PtCo-$Co(OH)_2$/C, PtCo-$Co(acac)_2$/C and PtCo-$Co(acac)_3$/C catalysts were synthesized by same method except for using different Co precursors of $Co(Ac)_2$, $Co(OH)_2$, $Co(acac)_2$ and $Co(acac)_3$. The ternary, quaternary and even quinary Pt_3Co-based catalysts were synthesized by adding 1/3 molar of corresponding metal precursors, including $Ni(acac)_2$, $Cu(acac)_2$, and $Zn(NO_3)_2{\cdot}6H_2O$. The synthetic conditions for home-made Pt/C (H-Pt/C) were similar to those of D-Pt_3Co/C except without adding Co precursor into the synthesis reaction. The decagram level D-Pt_3Co/C was produced with 4 g $Pt(acac)_2$, 1.3 g $2CoCO_3{\cdot}3Co(OH)_2$, 8 g Vulcan XC-72R carbon and 10 mL formaldehyde in 990 mL ethylene glycol solvent, and the other synthesis conditions and procedures are same to those of D-Pt_3Co/C.

1.4 Electrochemical measurements.

The electrochemical tests of catalysts refer to several articles labeled[1-3]. The electrochemical measurements for ORR were performed using a glassy-carbon Rotating Disk Electrode (RDE, Pine Research Instrumentation, diameter: 5 mm, area: 0.196 cm^2) connected to an installation of rotating electrode speed control (Pine Research Instrumentation, model: AFMSRCE). The saturated calomel electrode (SCE) and carbon rod were used as reference electrode and counter electrode, respectively. The prepared catalyst (2.5 mg) was dispersed in isopropyl alcohol and 5% Nafion solution to form the uniform catalyst ink with the help of ultrasound instrument. The amount of Pt is calculated according to the feed ratio, and the commercial catalyst is calculated according to the given mass fraction. 5 μL ink was dropped on the rotating disk electrode. The electrochemically active surface area (ECSA) of each catalyst was measured in 0.1 M $HClO_4$ solution at room temperature. The scanning range was 0.05-1.26 V *vs*. RHE. Activation scan of 10 cycles was carried out firstly at a scanning rate of 0.20 V/s. Then the cyclic voltammogram (CV) curve was carried out at the scanning rate was 0.05 V/s. By integrating the hydrogen adsorption area (0.05 ~ 0.40 V *vs*. RHE) within the sweep of CV curve, the ECSA value of catalyst can be calculated with the following equation.

$$ECSA\left(m^2 g_{Pt}^{-1}\right) = \int_{E1}^{E2} \frac{I[A]/v[V/s] \times dE[V]}{Q[C/m^2] \times M_{Pt}[g]}$$

Where I is the current, E is the potential, v is the scanning rate, E1 and E2 are the upper and lower

potentials corresponding to hydrogen adsorption on Pt, and Q is the charge density passing through hydrogen adsorption process. It was experimentally determined that the Q value of polycrystalline Pt used for ECSA calculations was 210 μC/cm^2, which represented the maximum hydrogen adsorption and was fairly close to the expected average for full surface coverage of dense Pt.

The ORR performance of each catalyst was studied by linear sweep voltammetry (LSV). The potential was scanned from 0 V to 1.20 V at a scanning rate of 0.01 V/s and a rotation rate of 1600 rpm in 0.1 M $HClO_4$ aqueous solution purged with the saturated O_2. The kinetic current (I_k), which represents the ORR activity of the catalyst, was calculated by Koutecky-Levich equation at 0.90 V *vs*. RHE.

$$\frac{1}{I} = \frac{1}{I_k} + \frac{1}{I_d}$$

Where I is the experimental measurement current, I_d is the diffusion limiting current, and I_k is the kinetic current. After the I_k kinetic current was calculated according to the formula, the kinetic current was normalized to the loaded metal and ECSA for each catalyst to obtain the mass activity and specific activity, respectively. The accelerated durability tests (ADTs) were performed at room temperature in 0.1 M $HClO_4$ solutions under a N_2 atmosphere by applying the cyclic potential sweeps between 0.6 and 1.1 V *vs*. RHE at a sweep rate of 100 mV/s for 30000 cycles.

1.5 MEA tests.

The membrane electrode assembly (MEA) performance of different catalysts were measured under the operating PEMFC conditions. Specifically, Pt_3Co/C and commercial Pt/C were dispersed in the solvent mixture of i-propanol, DI water, and 5% Nafion solution. Add 5% of the perfluorosulfonic acid solution to the mixture and weigh the amount of perfluorosulfonic acid in the solution according to I:C =0.7, where I is the mass of the perfluorosulfonic acid in the solution and C is the mass of the carbon in the catalyst. Homogenize the solution by ultrasonic instrument. The test was carried out on the 850G Auto MultiGas (AMG) Accessory with an 850E Fuel Cell Test System and the active area tested was 25 cm^2 (5 cm × 5 cm). The catalyst concentration was controlled to be 5-10 mg/mL. Catalysts are coated on both sides of the proton exchange membrane. Pt_3Co/C catalyst loaded 0.1 mg_{Pt}/cm^2 was used as the cathode and commercial Pt/C catalyst loaded 0.1 mg_{Pt}/cm^2 was used as the anode. The prepared CCM was dried to allow the solvent to evaporate completely. A gas diffusion layer (GDL) containing a microporous layer was used with a thickness of 180 μm and a pressure of 25 kPa. The MEA was obtained by pressing two GDLs, two gaskets and the prepared CCM. For H_2-air (or O_2) fuel cells, the anode and cathode were injected with pure hydrogen (99.999%, 500 mL/min) and air (or O_2, 99.999%) (1500 mL/min for air or

500 mL/min for O_2), respectively. The battery operated at 80°C and the relative humidity (RH) of both hydrogen and oxygen was 100% throughout the test. The backpressure of both anode and cathode is 50, 100, or 150 kPa. The MEA is activated to achieve a stable state prior to the performance testing.

The activation process was carried out at a backpressure of 100 kPa and the cell temperature of 80°C, with hydrogen and air at a flow rate of 500 mL/min. Before the polarization curves were recorded, the MEA was fully activated by holding at 0.60 V, 0.50 V, and 0.40 V for 5 min, 5 min, and 5 min for 5 cycles to stabilize the potential and current density. The process is then repeated until there is no significant difference between the two currents at the same voltage. The accelerated stress tests (ASTs) are conducted in accordance with DOE protocols of USA. The 100% humid hydrogen and nitrogen were passed through the anode and cathode, and the applied electric field was applied at 0.95 V and 0.60 V for 3 s potentiostatic scanning respectively.

Supporting Figures

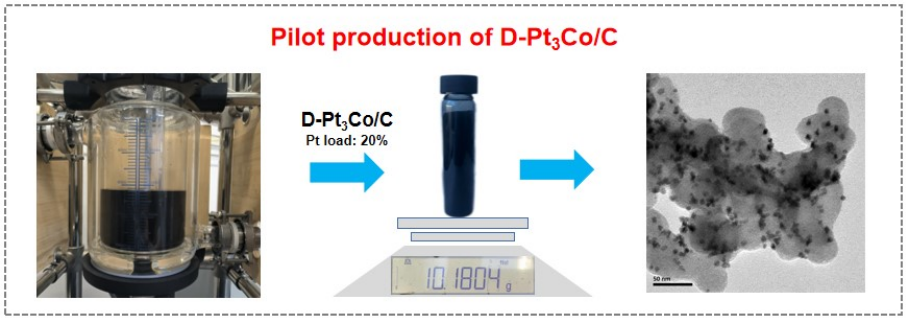

Figure S1. D-Pt_3Co/C pilot production device, production diagram and TEM image of synthesized D-Pt_3Co/C catalyst.

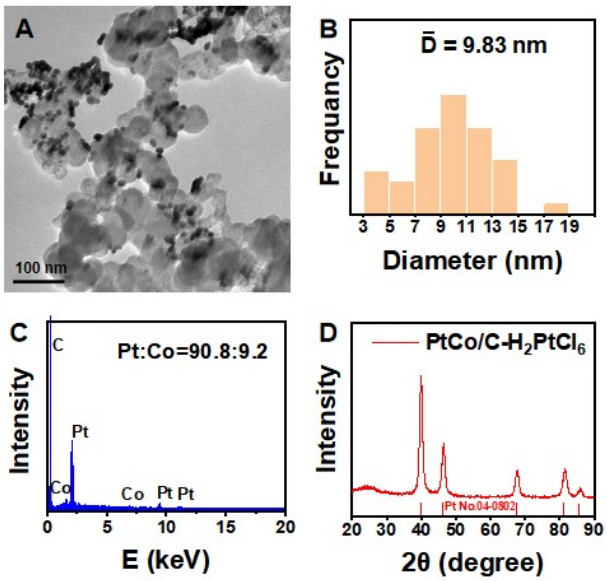

Figure S2. (**A**) TEM image, (**B**) particle size statistical diagram, (**C**) SEM-EDS, and (**D**) XRD pattern of PtCo/C-H_2PtCl_6.

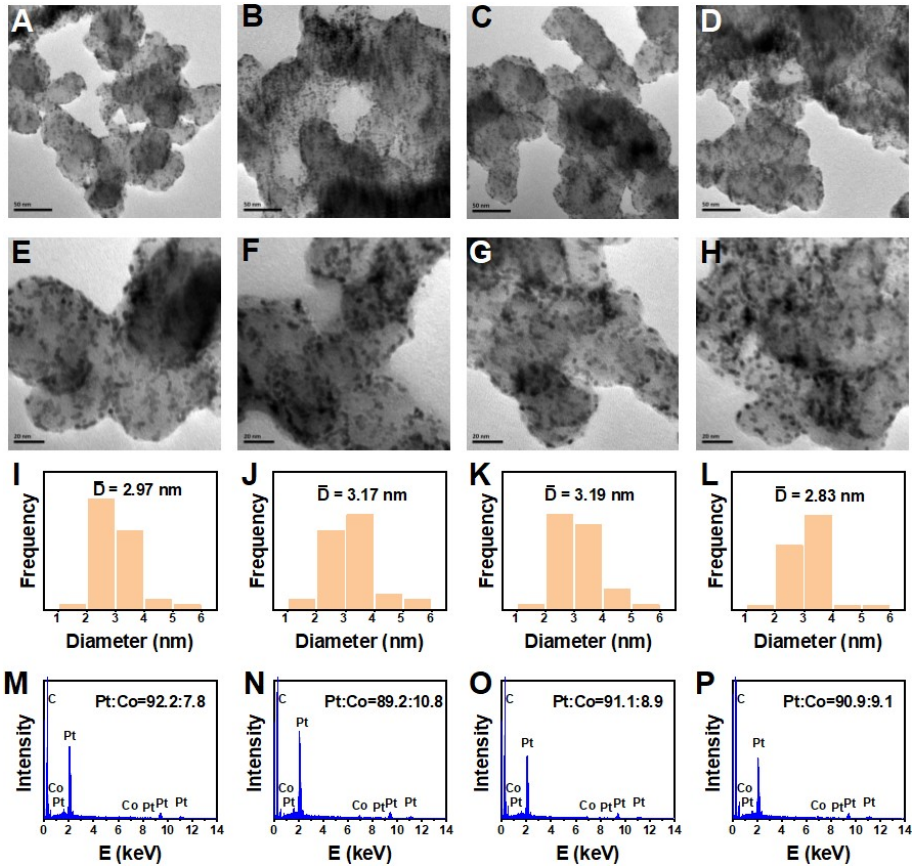

Figure S3. (**A-H**) TEM images, (**I-L**) particle size histogram statistics, and (**M-P**) SEM-EDS of different PtCo/C catalysts synthesized with different Co precursors: (**A, B, I, M**) $Co(Ac)_2$, (**C, D, J, N**) $Co(OH)_2$, (**E, F, K, O**) $Co(acac)_2$ and (**G, H, L, P**) $Co(acac)_3$.

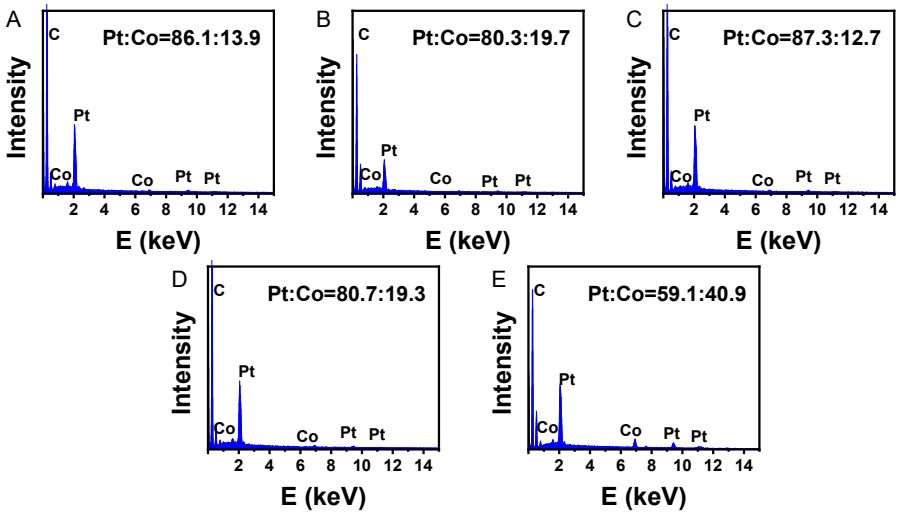

Figure S4. SEM-EDS of PtCo/C catalysts synthesized with different Co precursors before acid washing step: (**A**) $Co(Ac)_2$, (**B**) $Co(OH)_2$, (**C**) $Co(acac)_2$ and (**D**) $Co(acac)_3$ and (**E**) $2CoCO_3{\cdot}3Co(OH)_2$.

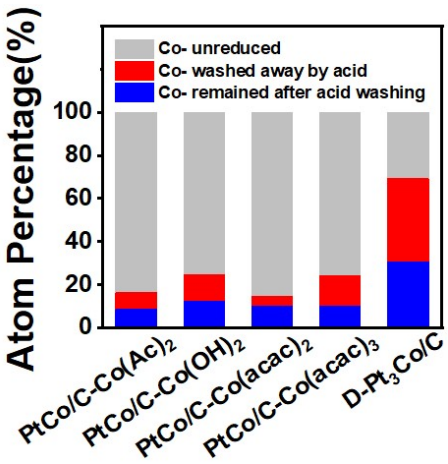

Figure S5. Histogram of Co atom percentages for PtCo/C catalysts synthesized with different Co precursors in different stages.

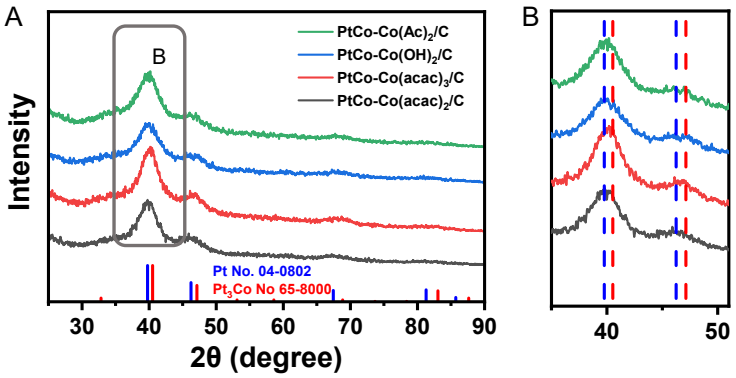

Figure S6. (**A**) XRD patterns of PtCo/C catalysts synthesized with different Co precursors. (**B**) Enlarged XRD patterns of the marked area in graph A.

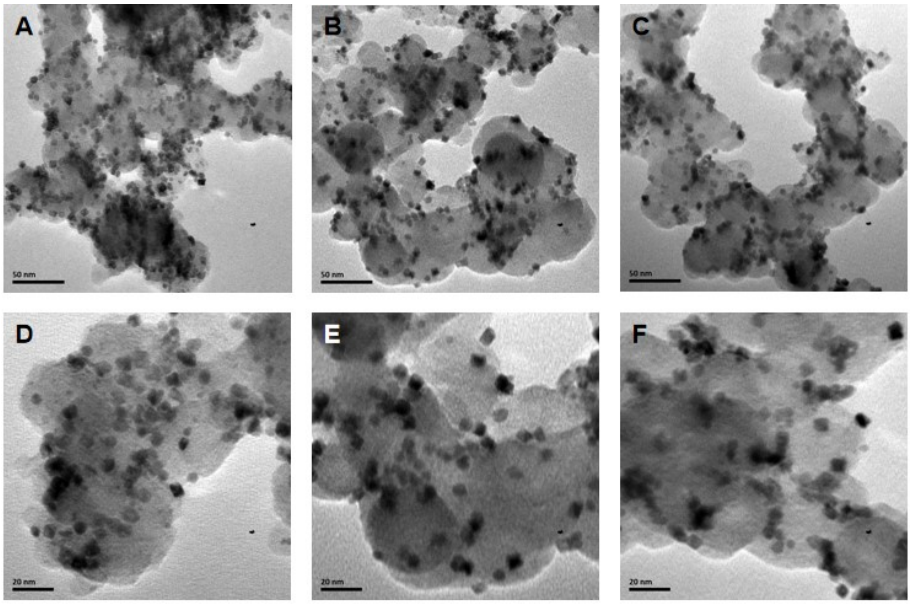

Figure S7. TEM images of D-Pt_3Co/C catalyst with different synthesis concentrations of (**A, D**) 20, (**B, E**) 40 and (**C, F**) 60 mg/mL.

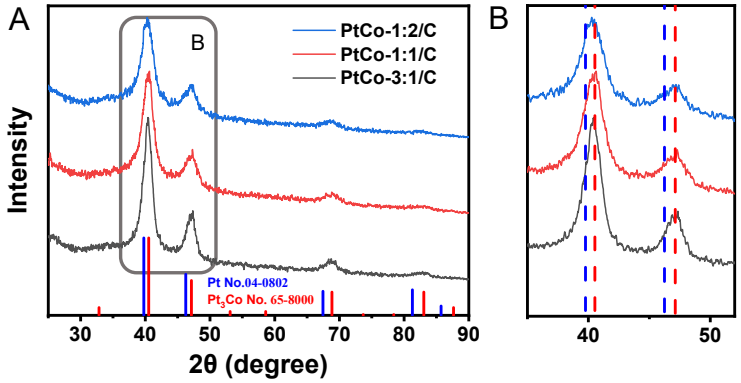

Figure S8. (**A**) XRD patterns of PtCo/C with different Pt/Co feeding ratios. (**B**) Enlarged XRD patterns of the marked area in graph **A**.

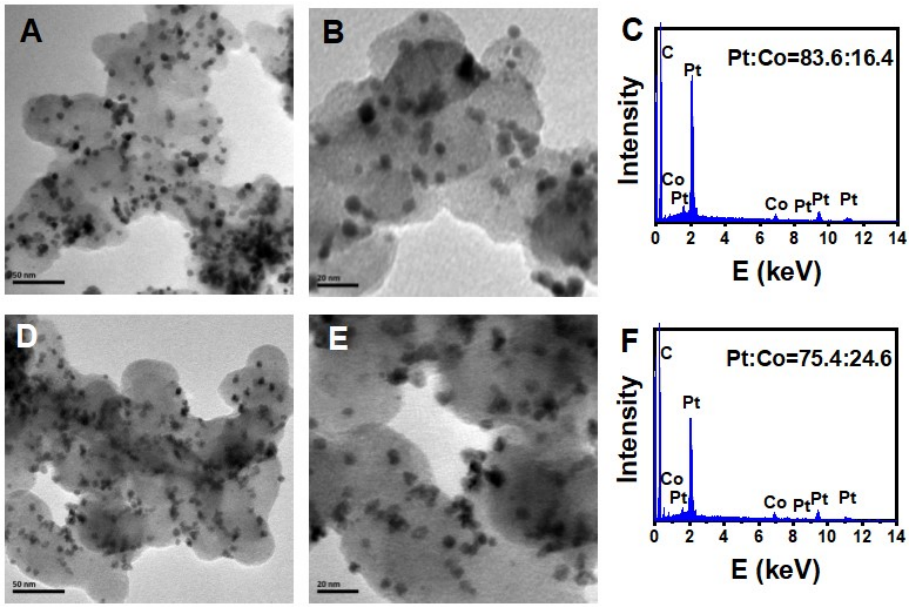

Figure S9. (**A, B**) TEM images and (**C**) SEM-EDS of PtCo/C with Pt/Co feeding ratios of 3:1. (**D, E**) TEM images and (**F**) SEM-EDS of PtCo/C with Pt/Co feeding ratios of 1:2.

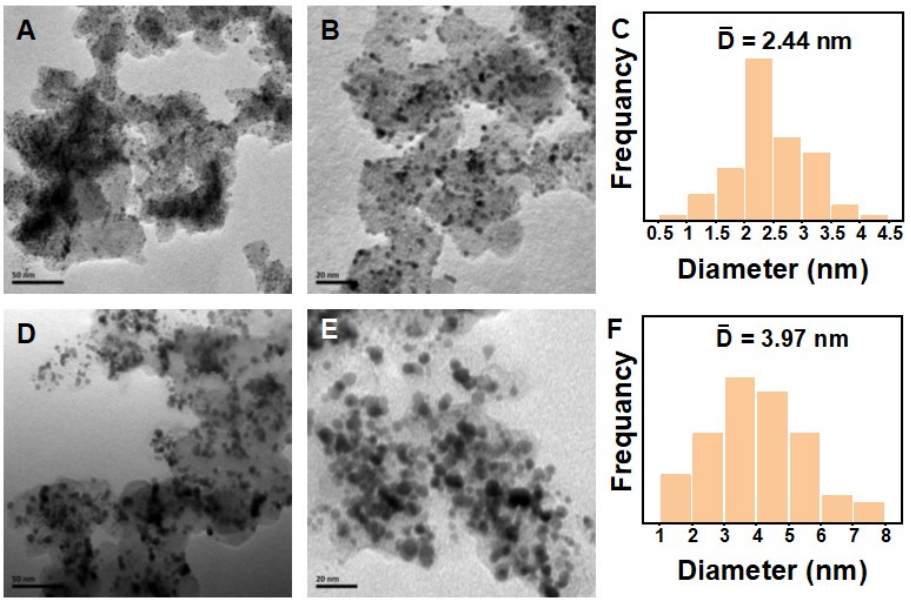

Figure S10. (**A, B**) TEM images and (**C**) particle size statistical diagram of C-Pt/C. (**D, E**) TEM images and (**F**) particle size statistical diagram of H-Pt/C.

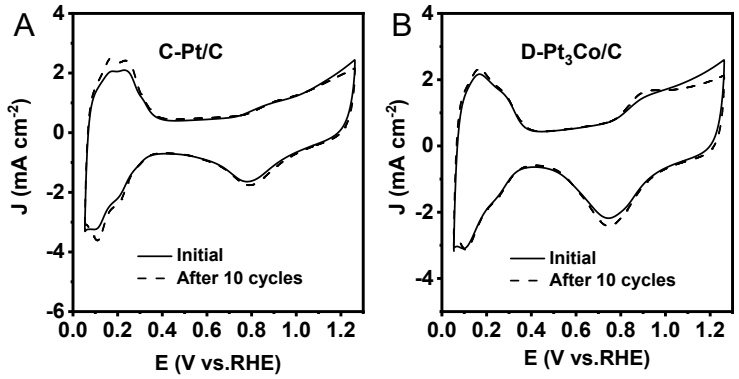

Figure S11. CV curves of (**A**) C-Pt/C and (**B**) D-Pt_3Co/C before and after 10 cycles activation measured at a sweep rate of 0.20 V/s in 0.1 M $HClO_4$.

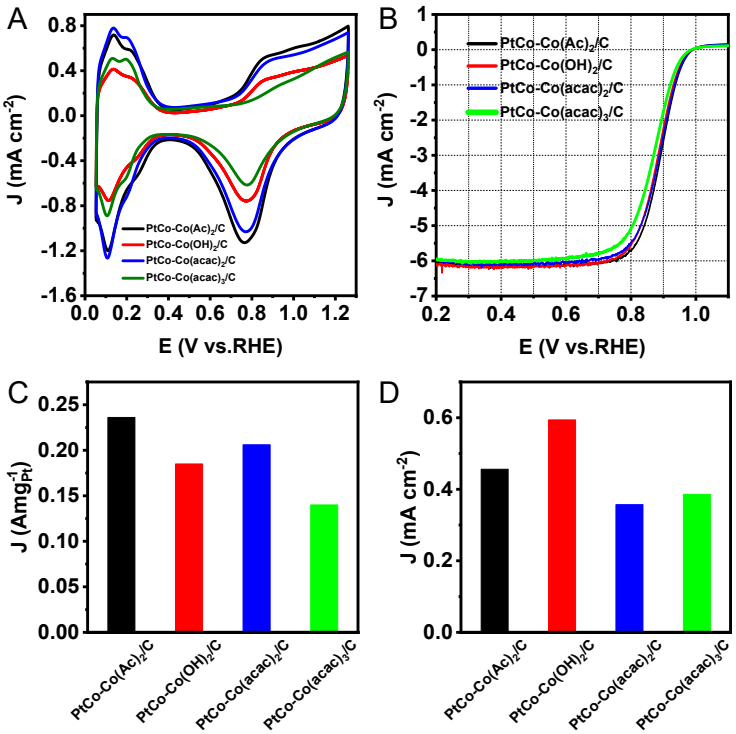

Figure S12. (**A**) CV curves in 0.1 M $HClO_4$, (**B**) ORR polarization curves in O_2-saturated 0.1 M $HClO_4$, and (**C**) mass activities and (**D**) specific activities at 0.90 V *vs*. RHE of different PtCo/C catalysts synthesized with different Co precursors.

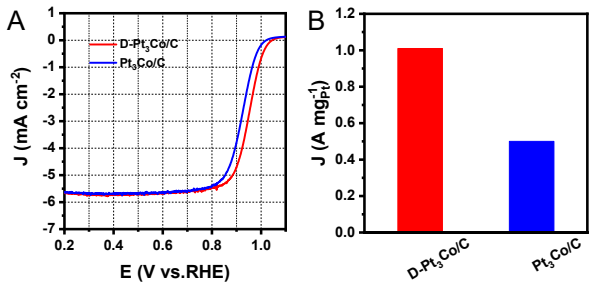

Figure S13. (**A**) ORR polarization curves in O_2-saturated 0.1 M $HClO_4$ and (**B**) mass activities at 0.90 V *vs*. RHE of D-Pt_3Co/C and Pt_3Co/C catalysts.

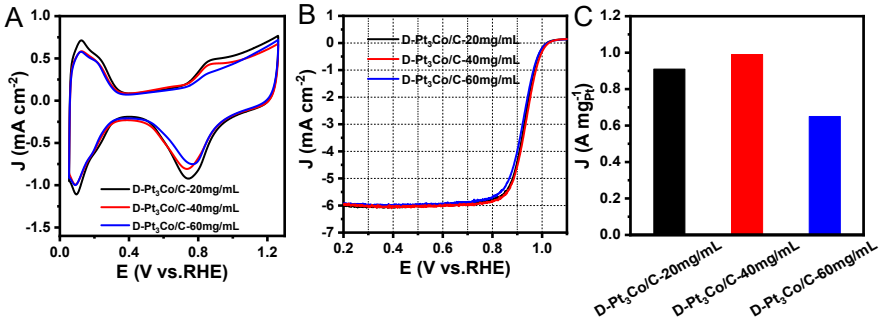

Figure S14. (**A**) CV curves in 0.1 M $HClO_4$, (**B**) ORR polarization curves in O_2-saturated 0.1 M $HClO_4$, and (**C**) mass activities at 0.90 V *vs*. RHE of different D-Pt_3Co/C catalysts.

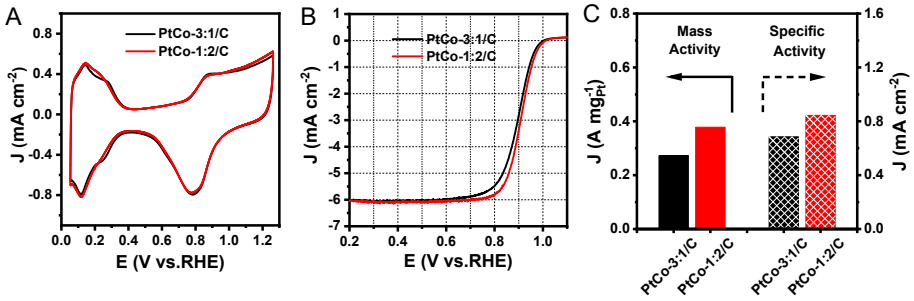

Figure S15. (**A**) CV curves in 0.1 M $HClO_4$, (**B**) ORR polarization curves in O_2-saturated 0.1 M $HClO_4$, and (**C**) mass activities and specific activities at 0.90 V *vs*. RHE of catalysts with different feeding ratios of Pt/Co.

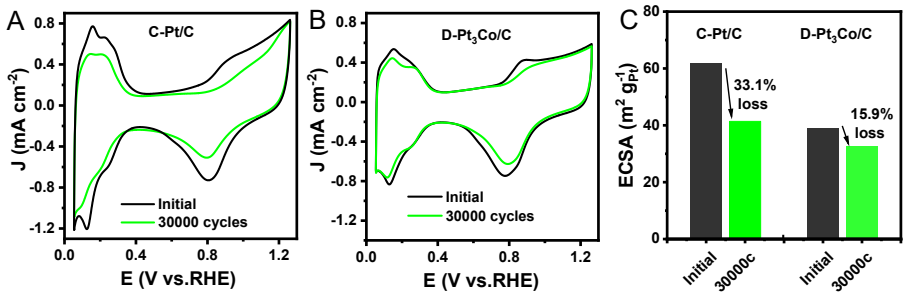

Figure S16. CV curves of (**A**) C-Pt/C and (**B**) D-Pt_3Co/C before and after 30000 cycles of ADTs. (**C**) The changes of ECSA for C-Pt/C and D-Pt_3Co/C before and after 30000 cycles of ADTs.

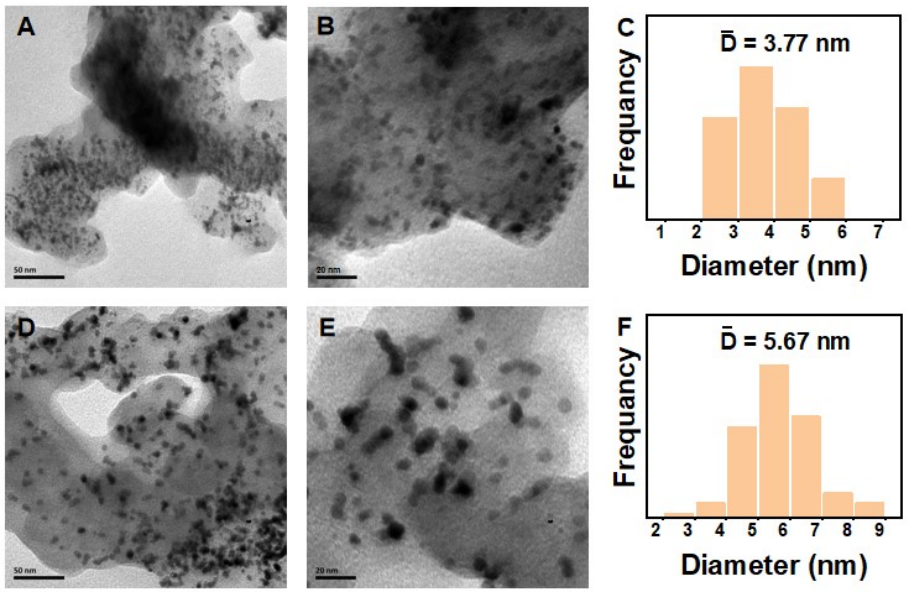

Figure S17. (**A, B**) TEM images and (**C**) particle size statistical diagram of C-Pt/C after 30000 cycles of ADTs. (**D, E**) TEM images and (**F**) particle size statistical diagram of D-Pt_3Co/C after 30000 cycles of ADTs.

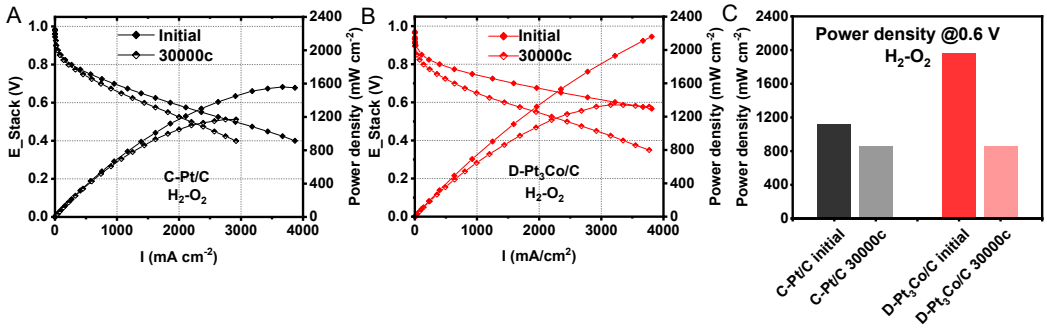

Figure S18. Polarization curves and power densities of (**A**) C-Pt/C and (**B**) D-Pt_3Co/C before and after 30000 cycles of ASTs. (**C**) Histogram of power densities for C-Pt/C and D-Pt_3Co/C before and after 30000 cycles of ASTs.

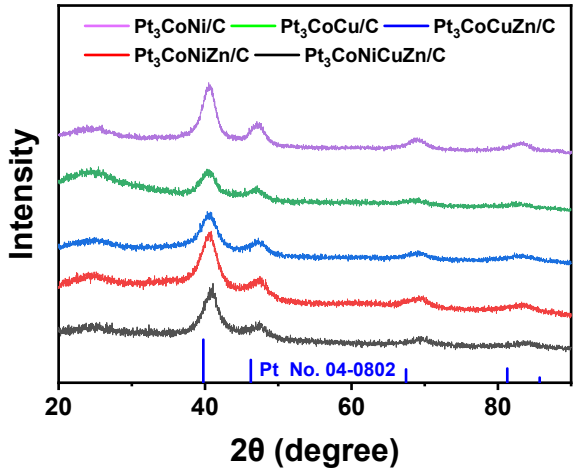

Figure S19. XRD patterns of a series of ternary, quaternary, and quinary Pt_3Co-based catalysts.

Reference

1. Huang, X. Q. High-performance transition metal-doped Pt_3Ni octahedra for oxygen reduction reaction. *Science* 2015, **348**, 1230-1234.
2. Bu, L. Z. Biaxially strained PtPb/Pt core/shell nanoplate boosts oxygen reduction catalysis. *Science* 2016, **354**, 1410-1414.
3. Cheng, H. Subsize Pt-based intermetallic compound enables long-term cyclic mass activity for fuel-cell oxygen reduction. *Proc. Natl. Acad. Sci. USA* 2021, **118**, e2104026118.